Comparative Medicine
Copyright 2020
by the American Association for Laboratory Animal Science

Vol 70, No 6
December 2020
Pages 492–498

Original Research

Effect of Xylazine–Tiletamine–Zolazepam on the Local Field Potential of the Rat Olfactory Bulb

Peter Olegovich Kosenko,* Aleksey Borisovich Smolikov, Viktor Borisovich Voynov, Pavel Dmitrievich Shaposhnikov, Anton Igorevich Saevskiy, and Valeriy Nikolaevich Kiroy

Neural oscillations of the mammalian olfactory system have been studied for decades. This research suggests they are linked to various processes involved in odor information analysis, depending on the vigilance state and presentation of stimuli. In addition, the effects of various anesthetics, including commonly used ones like chloral hydrate, pentobarbital, ketamine, and urethane, on the local field potential (LFP) in the olfactory bulb (OB) have been studied. In particular, the combination of xylazine and tiletamine–zolazepam has been shown to produce steady anesthesia for an extended period and relatively few adverse effects; however, their effects on the LFP in the OB remain unknown. To study those effects, we recorded the LFP in the OB of rats under xylazine–tiletamine–zolazepam anesthesia. During the period of anesthesia, the spectral powers of the 1–4, 9–16, 31–64, 65–90 frequency bands increased significantly, and that of 91–170 Hz frequency band decreased significantly, whereas no significant changes were observed in the 5–8 and 17–30 Hz ranges. These results reveal dynamic changes in the time and frequency characteristics of the LFP in the OB of rats under xylazine–tiletamine–zolazepam anesthesia and suggest that this combination of anesthetics could be used for studying oscillatory processes in the OB of rats.

Abbreviations: KX ketamine-xylazine; LFP, local field potential; OB, olfactory bulb; TZ, tiletamine-zolazepam; XTZ, xylazine-tiletamine-zolazepam

DOI: 10.30802/AALAS-CM-20-990015

Sensory systems provide the brain with accurate information about the external world. In unanesthetized animals, sensory networks are modulated by changes in vigilance states that are influenced by various processes including cognitive, attentional, arousal, and emotional states and previous experiences.[10,12] Anesthesia is induced by drugs that target neuromodulating systems of the brain. Many anesthetic drugs are used in medicine and research, but even for the most commonly used ones, their effects on neural network activity are poorly understood. The effects of the most popular noninhalational drugs, including chloral hydrate, pentobarbital, urethane, and ketamine, on the local field potential (LFP) of the olfactory sensory system have been studied over the past several years.[8,11,13,36] This research has shown that chloral hydrate and pentobarbital significantly reduce the power of fast-θ (5 to 12 Hz) oscillations without affecting slow-θ (1 to 4 Hz) activity, whereas urethane significantly increases slow-θ activity but reduces fast-θ oscillations.[36] In addition, chloral hydrate and pentobarbital significantly increase whereas urethane and ketamine significantly and sharply reduce the power of β-oscillations.[8,36] The γ range is usually divided into 2 subranges (31 to 64 Hz and 65 to 90 Hz), which are proposed to have different roles in recognition of smells.[25,36,47] The power of both subranges fell immediately after the administration of chloral hydrate, pentobarbital, and urethane; γ power slowly returned to baseline after the injection of chloral hydrate or pentobarbital, but no recovery was observed for urethane anesthesia.[36] Spontaneous γ activity was greatly reduced under urethane anesthesia, and no bursts associated with the respiratory rhythm were observed.[1,36] Ketamine also reduced the power of both γ subbands, but unlike other types of anesthesia, ketamine induced a shift in γ frequency from 60 to 90 Hz to 100 to 130 Hz in mice.[8]

Tiletamine–zolazepam (TZ) is a commonly used anesthetic combination. Like ketamine, tiletamine hydrochloride is an antagonist of N-methyl-d-aspartate receptors. TZ has a rapid pharmacologic effect, is a proven muscle relaxant, and maintains high oxygen saturation of arterial hemoglobin, thus making this drug ideal for veterinary clinical research and for various minor surgical procedures in domestic and wild animals.[18,29,37,54] Because of its rapid absorption, TZ achieves an effective level of anesthesia with little cardiopulmonary inhibition and has a wide margin of safety in terms of tolerance in animals.[39] The main disadvantages of TZ are a prolonged recovery period and lack of strong and specific antagonists that reverse the drug-induced inhibition of cardiopulmonary functions, adverse effects such as anxiety and spontaneous movements,, or prolonged recovery from anesthesia.[38] TZ is recommended for use in conjunction with xylazine, which is an α2 adrenergic agonist.[30]

This study is the first to evaluate the effects of xylazine–tiletamine–zolazepam (XTZ) on the dynamics of bioelectrical activity of neural networks in the olfactory bulbs (OB) of rats and indicates that the effects of XTZ should be considered when studying oscillatory processes in rat OB

Received: 06 Feb 2020. Revision requested: 21 Apr 2020. Accepted: 19 Aug 2020.
Southern Federal University, Rostov on Don, Russia
**Corresponding author. Email: peza-i@mail.ru*

Materials and Methods

The experiments involved 8 adult male Norway rats (*Rattus norvegicus*; weight, 350 to 450 g), which were housed in individual microisolators (54 cm × 39 cm × 21 cm, with sawdust bedding) under constant temperature (23 ± 1 °C) and humidity and a 12:12-h light:dark cycle. Rats had free access to food (Complete extruded combo feed for laboratory animals, JSC Gatchinskiy compound feed plant) and reverse-osmosis purified water. All experimental and animal care procedures were approved in advance by the animal ethics committee of Southern Federal University (Rostov on Don, Russia).

Surgery. Rats were anesthetized by intramuscular injection of TZ (30 mg/kg; Zoletil, Virbac Lab, Carros, France) and xylazine (6 mg/kg; Interchemie Werken de Adelaar, Venray, Netherlands) and placed in a stereotaxic frame (SR-6M-HT, Narishige, London, United Kingdom). After a midline scalp incision, 5 small holes were drilled in the cranium to insert surgical screws for anchoring, and a larger hole was drilled over the left OB (0 to 1.5 mm mediolateral and 7.0 to 10.0 mm anterioposterior to bregma) for implantation of a microelectrode array. After opening of the dura, the array of microelectrodes (2 rows of 8 electrodes, with an interelectrode distance of 500 µm) was inserted into the glomerular layer of the OB at a depth of approximately 100 µm below the surface of the brain. Recording sites were confirmed through histologic examination of the brain after euthanasia. The wire implanted in the space between the skin and nose bone was used as a ground. Five anchor screws and the array of microelectrodes were attached to male pins that were shaped in a rectangular 2 × 4 socket array and secured with dental acrylic cement to the skull. All above mentioned surgical procedures were performed under sterile conditions.

During the postoperative period, rats received an intramuscular carprofen injection (4 mg/kg; Rimadyl, Zoestis Pet Care, Parsippany, NJ) daily for 5 d. The wound was washed daily for 4-5 days by rinsing with chlorhexidine (Tula Pharmaceutical Factory LLC, Russia) and then Oflomelide ointment was applied (Joint-Stock Kurgan Society of Medicines and Products Sintez, Russia). After surgery, the rats were assessed daily by monitoring their behavior and weight. Rats received at least one week to recover from surgery before beginning the experiments.

LFP recording. LFP recording was performed in a rectangular chamber (100 cm × 50 cm) inside a Faraday cage. LFP was recorded and digitalized by using a 32-channel data acquisition system (Multichannel Acquisition Processor, Plexon, Dallas, TX) with a sampling frequency of 10 kHz. The information was saved in the hard drive of a host computer.

On the day of the experiment, rats were habituated to the recording environment for at least 30 min, after which 60 min of baseline activity was recorded. After intramuscular injection of xylazine–tiletamine–zolazepam (XTZ; 17 mg/kg Zoletil and 5 mg/kg xylazine), recording of the OB LFP in anesthetized rats was continued for at least 120 min. To avoid circadian effects, all experiments began at approximately the same time (1000), and rats were fully awake during all baseline recording. The rationale for choosing this recording duration was to allow the capture of the maximal amount of information during the anesthesia induced by the given dose of the anesthetic; after approximately 110 to 120 min, rats began to demonstrate behavior indicating the start of recovery from anesthesia.

Statistical analysis. LFP signals were analyzed by using the software program NeuroExplorer4 (Nex Technologies, Colorado Springs, CO). The total LFP data were divided into segments, each containing 10 min of data. During visual inspection of the recorded OB LFP, high-amplitude bursts related to animal movement, considered to be artifacts, were excluded from further analysis. After exclusion of artifacts, power spectral density analysis was performed by segment (Hanning window; FFT size, 512; frequency resolution, 0.41 Hz), and the spectral power was calculated for each frequency resolution. In our study, LFP signals were divided into 3 main frequency bands of oscillations: θ oscillations (1–4, 5–8, and 9–16 Hz), β oscillations (17–30 Hz), and γ oscillations (31–64, 65–90, and 91–170 Hz). To examine the effect of the anesthetic combination on oscillations, baseline power was calculated by using the 10 min of data collected just before anesthetic injection.

All statistical analyses were performed by using Sigma Plot 11 (Systat Software, Santa Clara, CA) and Excel (Microsoft, Redmond, WA). Data were assessed for significance by using one-way ANOVA followed by the Tukey posthoc multiple-comparison test. Values are given as mean ± SEM. A P value of less than 0.05 was considered significant.

To obtain the dominant frequencies in the γ band (that is, those with the highest spectral powers), the following procedure was performed on the OB bioelectrical activity–time series: 1) split the series into 1-min bins, 2) apply the Welch method (parameters used: Hanning window, window length of 1024, and a 50% windows overlap)[53] to each of the bins for obtaining the corresponding power spectra), and 3) determine the frequency with the highest power in the γ band for each bin, thereby forming the final time series for dominant γ frequencies. Afterward, linear regression analysis was performed on the resulting series to calculate corresponding coefficients and R2 scores. The procedures were all performed by using the packages Scipy, Numpy, and Scikit-learn for Python programming language.[21,23,46,52]

Results

General effect of XTZ on the OB of rats Before anesthesia, the behavior of rats in their experimental cage was characterized as exploratory or quiet waking, and LFP signals recorded from the glomerular layer of OB were typical for this state, comprising low-amplitude signals that included slow (1–4 Hz) and low-amplitude fast (30–170 Hz) waves. By 10 min after the administration of XTZ, the LFP had changed dramatically, demonstrating increased high-frequency (91–170 Hz) oscillations, which were observed consistently until 110 to 120 min after anesthesia induction (Figures 1 and 2).

Effect of XTZ on the spectral characteristics of rat OB LFP. To quantitatively analyze the effects of the XTZ on the oscillations of OB, we used the relative energy power of the oscillations as an index for further analysis. We first focused on θ oscillations (1–8 Hz), which we further divided into 2 subbands: 1–4 Hz, corresponding to the respiratory rhythm during the anesthetized or awake stationary state, and 5–8 Hz, corresponding to the exploratory state.[6]

After administration of the XTZ mixture, the power of the 1–4-Hz subband increased slowly and was significantly different from baseline during the 50 to 80 min interval, after which it returned to the baseline level (ANOVA; $F_{12,101} = 4.824$; multiple-comparison; $P < 0.05$ for 50, 60, 70, and 80 min; $n = 8$; Figure 2). No significant changes were seen in the spectral power of the 5–8-Hz subband (ANOVA; $F_{12,101} = 2.616$; multiple-comparison; all $P > 0.05$; $n = 8$; Figure 2). After drug administration, the difference in the power of the 9–16-Hz band compared with baseline reached significance between 20 and 50 min (ANOVA; $F_{12,101} = 7.940$; multiple-comparison; $P < 0.05$ for 20, 40, and 50 min; $n = 8$; Figure 2) and thereafter returned to the baseline level. XTZ anesthesia had no significant effect on the spectral power at 17

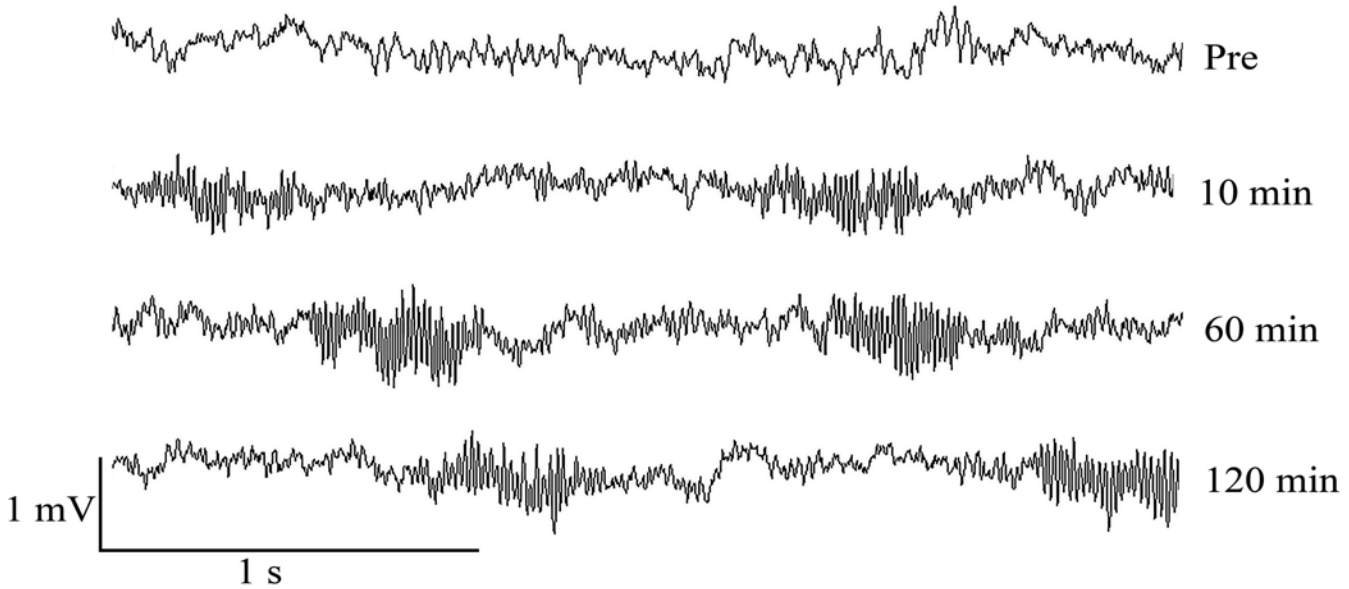

Figure 1. General effects of xylazine–tiletamine–zolazepam on the raw data of the LFP signal from rat OB. Pre, LFP data obtained before the application of anesthetics; post, 10 to 120 min after the application of anesthetic.

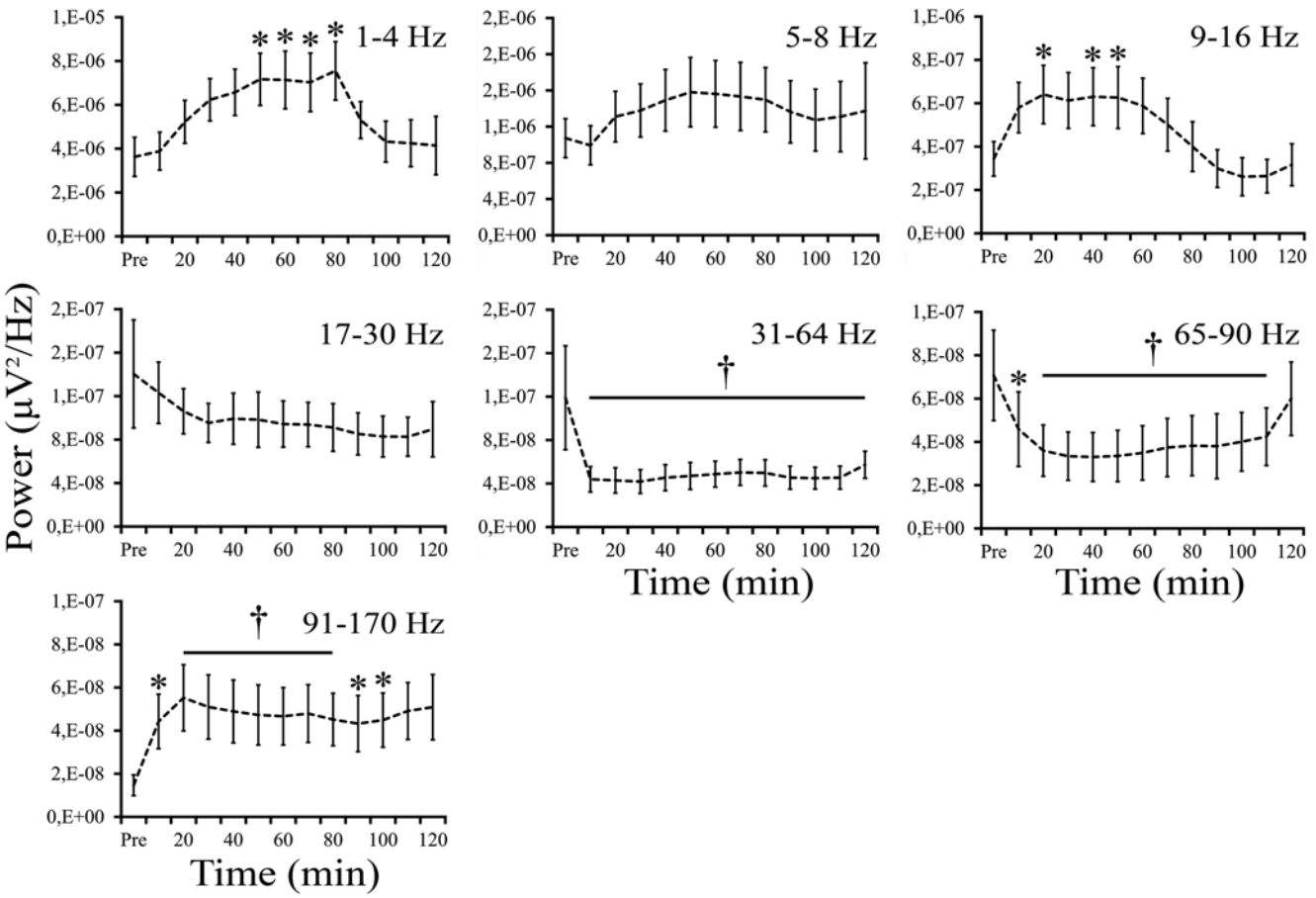

Figure 2. Effects of xylazine–tiletamine–zolazepam on the spectral power of the LFP signal from rat OB. Pre, LFP power data before the application of anesthetics; post, 10 to 120 min after the application of anesthetic. Left panel (top to bottom): 1 to 4 Hz, 5 to 8 Hz, 9 to 16 Hz, and 17 to 30 Hz; right panel (top to bottom), 31 to 64 Hz, 65 to 90 Hz, and 91 to 170 Hz; ∗, $P < 0.05$; †, $P < 0.01$.

to 30 Hz (ANOVA, F[12, 101] = 1.509; paired comparison, all $P > 0.05$; $n = 8$; Figure 2), which had high interindividual variability.

The γ oscillations of rodent OB play several roles in olfactory function.[26] We divided γ oscillations into 3 subbands: 31 to 64 Hz, 65 to 90 Hz, and 91 to 170 Hz. After XTZ injection, the power of the LFP in the 31–64-Hz band fell to 62% ± 12% of that of the preanesthesia period; these changes were significant for the entire time period (ANOVA; $F_{12,101} = 3.391$; multiple-comparison;

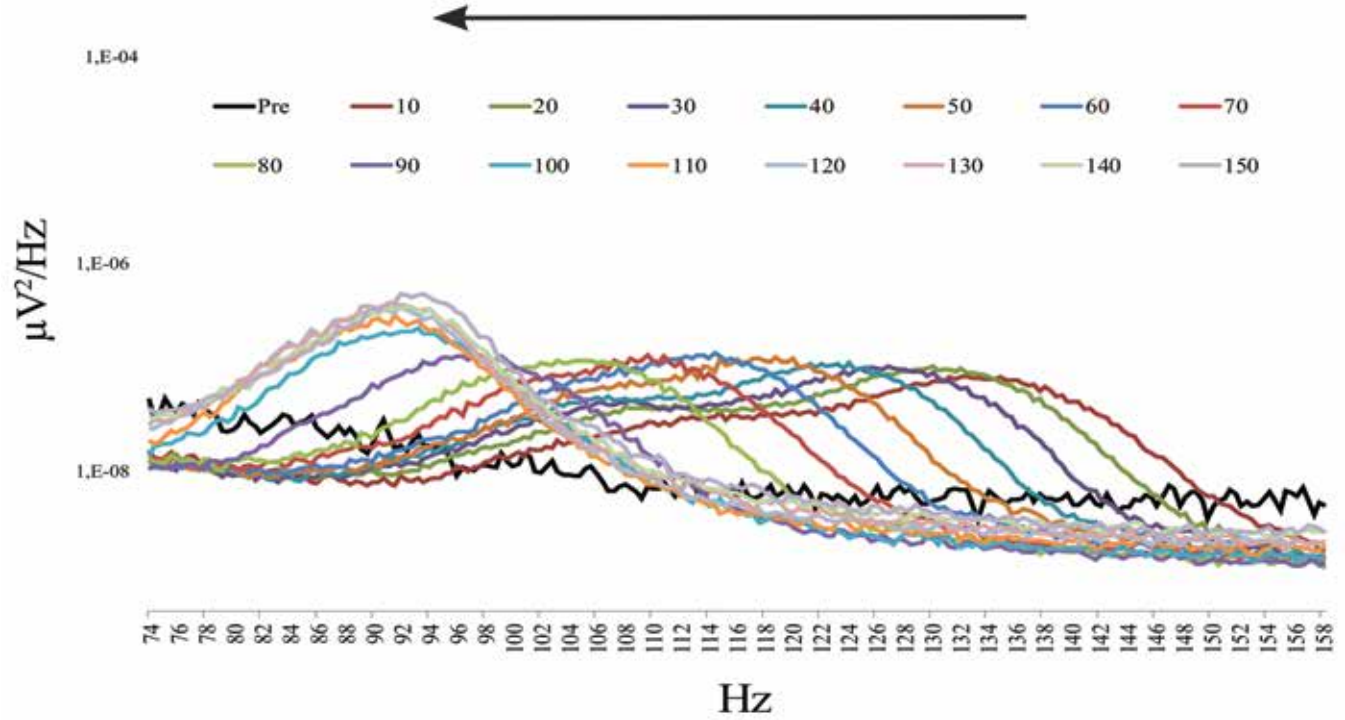

Figure 3. Effects of xylazine–tiletamine–zolazepam on the spectral characteristics of the LFP in rat OB. Pre, spectrogram calculated before the application of anesthetic; times from 10 to 150 min refer to the period after anesthetic application. The black arrow indicates the shift in the leading γ frequency during the time course.

all $P < 0.01$; $n = 8$; Figure 2). Similar changes were observed for the power of the subband of 65 to 90 Hz, which fell immediately after XTZ injection (Figure 2) and did not appear to recover until 110 min after XTZ administration (ANOVA; $F_{12,101} = 4.432$; multiple-comparison, all $P < 0.01$ [except for 10 min, $P < 0.05$]; $n = 8$; Figure 2). After 110 min, the LFP power returned to the baseline level. The biggest changes in the LFP after the administration of the XTZ mixture occurred in the subband 91 to 170 Hz. The power of the γ oscillations in this band increased significantly during first 10 min to about 4-fold greater than that during the preanesthetic period (ANOVA, $F_{12,101} = 3.118$; multiple-comparison, $P = 0.015$; $n = 8$; Figure 2) and remained higher throughout the observation period (ANOVA; $F_{12, 101} = 3.118$; multiple-comparison; $P < 0.01$ for 20, 30, 40, 50, 60, 70, and 80 min and $P < 0.05$ for 90 and 100 min; $n = 8$; Figure 2). The LFP power in the 91–170-Hz band remained elevated even at 150 min after XTZ administration, when rats had started to move slightly.

Effect of XTZ anesthesia on spectral characteristics of the γ oscillations of the LFP of rat OB. After XTZ administration, the dominant frequency of γ oscillations shifted from higher to lower frequencies (Figure 3). At 10 min afterwards, γ oscillations in LFP signal began to appear, with a dominant frequency of about 135 Hz. Over the time of the XTZ anesthesia, the dominant frequency was shifting to lower values. On an average of 100 min after XTZ administration, the shifting stopped, and the dominant frequency remained stable until 150 min after XTZ administration. In some cases, the dominant frequency of γ-oscillations shifted to lower frequency values in 120 min.

We observed different patterns of decrease and recovery of the dominant γ-frequency among our 8 subjects. For 6 rats, the pattern at the top of Figure 4 emerged and can be described as steep linear decrease followed by a shallow linear decrease, and then recovery. However, the remaining 2 rats demonstrated a strictly linear decrease until the end of the recording period (Figure 4, bottom).

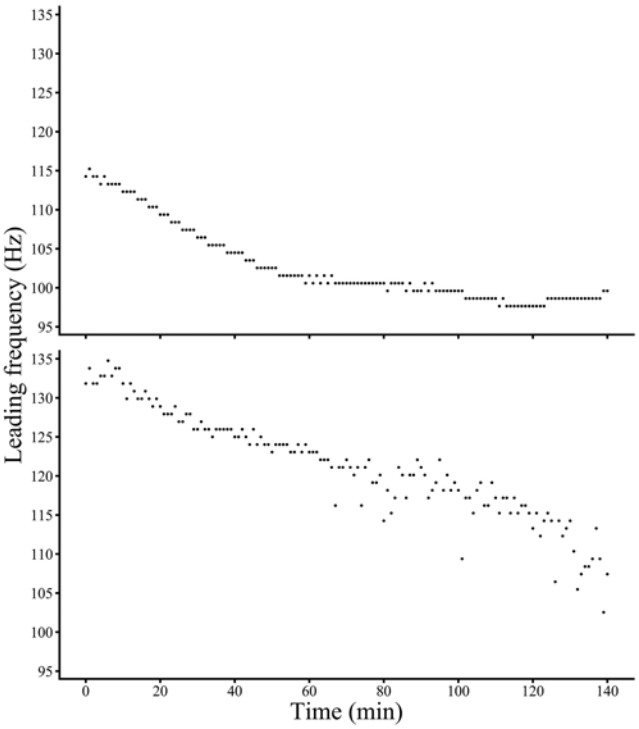

Figure 4. Time-associated effects of xylazine–tiletamine–zolazepam on γ oscillations of rat OB. The upper and lower panels of the figure contain examples of 2 different types of changes in the leading frequency γ activity. Each panel of the figure displays individual changes in the γ-band leading frequency of the olfactory bulb LFP.

The results of linear regression and initial linearity duration analysis are summarized in Table 1. Based on the value of the determination coefficient (R^2), most of the initial decreases in

Table 1. Results of linear regression and initial linearity duration analysis

Subject	Slope	Determination coefficient (R^2)	Linearity duration (min)
1	−0.32	**0.96**	110
2	−0.15	**0.99**	160
3	−0.25	**0.98**	65
4	−0.42	**0.99**	110
5	−0.38	0.76	70
6	−0.19	**0.93**	110
7	−0.27	**0.97**	95
8	−0.16	**0.90**	140
Mean	−0.27	0.94	107.50
SEM	0.10	0.08	32.07

Determination coefficients exceeding 0.9, that is, corresponding to nearly functional linear dependences, are marked bold.

dominant γ frequencies (6 of 8) were sufficiently linear to indicate dependence of dominant γ frequency on time. The linear regression coefficient (slope) did not change much, but the variation that was observed is possibly explained by inter-subject differences.

Discussion

The principles of the generation and the functional role of the rhythms in the LFP of the OB have recently been studied extensively,[16,26,44,47] especially those related to external olfactory stimuli and certain types of brain activity, like anesthesia.[14-17,27,28] The γ oscillations of the 31–64- and 65–90-Hz frequency bands are generated in the local neural circuits of OB, which consist of mitral (or tufted) and granule cells.[3,26,32,45,47,49] Those cells receive the modulating influence from sensory stimulations, including inhalation, and descending signals from different brain structures, particularly from nuclei raphes,[24] the piriform cortex,[42] and entorhinal cortex.[7]

Comparative analysis has revealed that the effects related to olfactory stimulation are expressed more clearly in LFP of the OB of anesthetized animals.[33] Moreover, OB LFP are highly efficient for qualitative and quantitative description of the stages of anesthesia, which is important for developing automated control of the anesthesia level during surgery in humans.[2] These findings demonstrate the relevance of studying OB LFP under anesthesia.

Zoletil combines 2 substances: tiletamine and zolazepam.[31] Like ketamine, tiletamine is an antagonist of N-methyl-D-aspartate receptors, whereas zolazepam modulates the activity of GABAa receptors, thus attenuating neuronal excitability.[19] The way in which TZ influences neurochemical structures has pronounced similarity with that of such anesthetics as chloral hydrate, pentobarbital, urethane, and ketamine.[5,8,9,30,34,35,41,45] The application of those anesthetics has been shown to increase spectral power in the 1–4-Hz frequency band and decrease power in the 30–90 Hz band in the OB.[36] A decrease of γ power in the 30–90-Hz range is considered as evidence of reduced neuronal excitability in OB and attenuated synaptic transmission.[43,50,51] KX anesthesia is known to efficiently suppress the spontaneous activity of mitral cells; however, in mice under the same conditions, high-frequency (exceeding 100 Hz) activity was enhanced.[8]

Our current study of rats showed that an XTZ mixture induced a significant increase of the OB γ activity in the 91–170-Hz frequency range, with maximal effect during the first 10 min after application. Compared with wakefulness, the power of those frequencies in OB LFP increased 4 times or more and were persistently higher throughout anesthesia, sometimes for as long as 150 min after a single injection. As anesthesia progressed, the modal value of the power distribution of this activity typically shifted toward the low-frequency spectrum, but even after 150 min, the modal value was not less than 90 Hz.

Because frequencies higher than 100 Hz have not been described in the LFP of rat OB, their formation conditions, generation mechanisms, and functional significance are unknown. The most probable suggestion is that this type of activity is related to the neuronal circuits of OB, which include mitral and granule cells, and is generated during wakefulness in the 60–90-Hz range; a shift in the 91–170-Hz range occurs when XTZ anesthesia blocks the descending (predominantly inhibiting) afferents. In this case, the mechanism for generating the high-frequency γ activity that we registered in our study might be related mostly to dendrodendritic synapses between mitral and granule cells, which are known to be the main source of γ activity.[47] Another, independent mechanism could also generate γ oscillations with frequency in 91–170-Hz in relation to GABA receptors. This potential mechanism may be suppressed during wakefulness or various types of anesthesia via descending inhibitory afferents but could be disinhibited under XTZ anesthesia, given that the γ-frequency power, as previously demonstrated for KX anesthesia, increases in OB LFP.[8] In addition, inhibition of GABA receptors in isolated hippocampal sections induced high-frequency (100 to 150 Hz) γ activity.[22]

The mechanism of action of TZ anesthesia is similar to that of ketamine[4] and produces functional disorganization of the limbic and thalamocortical systems.[20] Limbic and nonspecific thalamocortical structures play substantial roles in the promotion and maintenance of vigilance states in the sleep–wake cycle.[48] Anesthesia-associated disorganization of the activity of those structures can induce generalized sedative effects, including decreases in muscle tone and heart rate and variability of respiratory rhythm. Those changes occur during the first 30 to 60 s after intramuscular injection of the drug. At the same time, the excitability of OB, especially the mitral cells, does not decrease during anesthesia, but, on the contrary, increases;[43] as evidence, the presentation of odorants exerts a more pronounced effect during anesthesia than in wakefulness. This effect might be related to a weakened descending afferent signaling to the mitral and granule cells that is produced predominantly by inhibitory interneurons of OB.

The functional significance of high-frequency (>100 Hz) is unknown. The OB γ activity at 65 to 90 Hz and 91 to 170 Hz can contribute to the scanning mechanism for forming temporal windows for efficient processing of olfactory signals.

The purpose of our study was to examine the effect of XTZ anesthesia on OB LFP in rats. The most prominent effect was the appearance of high-frequency γ activity in OB LFP, as compared with that described earlier (including for other types of anesthesia), namely the γ activity of 91 to 170 Hz, in which spectral power substantially exceeded that of slow γ oscillations.[36] The activity at 91 to 170 Hz was clearly apparent during the first 10 min of anesthesia, whereas the modal value in the spectral power of this activity decreased almost linearly throughout anesthesia until 150 min, at which time its value was equal to that of the upper level of 65–90-Hz band. Considering the mechanism of action of XTZ anesthesia, we propose that such rhythm is typical for the local neuronal circuits of OB, win which mainly inhibitory descending afferents are attenuated. Given the previously demonstrated relationship between rhythmic activity in the OB with phases of anesthesia and sleep,[33,40] the mechanisms of synchronized activity generation in OB at the 91–170-Hz range and the role of this activity in the processing of olfactory information require further investigation.

Acknowledgment

This work was supported by the Foundation for Advanced Research of Russia (1 November 2017; number 6/112/2017–2020).

References

1. **Aylwin ML, Aguilar GA, Flores FJ, Maldonado PE.** 2009. Odorant modulation of neuronal activity and local field potential in sensory-deprived olfactory bulb. Neuroscience **162:**1265–1278. https://doi.org/10.1016/j.neuroscience.2009.05.051.
2. **Bagur S, Lacroix MM, de Lavilléon G, Lefort JM, Geoffroy H, Benchenane K.** 2018. Harnessing olfactory bulb oscillations to perform fully brain-based sleep-scoring and real-time monitoring of anaesthesia depth. PLoS Biol **16:**1–32. https://doi.org/10.1371/journal.pbio.2005458. .
3. **Bathellier B, Lagier S, Faure P, Lledo PM.** 2006. Circuit properties generating gamma oscillations in a network model of the olfactory bulb. J Neurophysiol **95:**2678–2691. https://doi.org/10.1152/jn.01141.2005.
4. **Berry SH.** 2015. Injectable anesthetics, p 277–296. Chapter 15. In: Grimm KA, Lamont LA, Tranquilli WJ, Greene SA, Robertson SA, editors. Veterinary anesthesia and analgesia: the 5th ed of Lumb and Jones. Ames (IA): Wiley–Blackwell.
5. **Buonviso N, Amat C, Litaudon P, Roux S, Royet JP, Farget V, Sicard G.** 2003. Rhythm sequence through the olfactory bulb layers during the time window of a respiratory cycle. Eur J Neurosci **17:**1811–1819. https://doi.org/10.1046/j.1460-9568.2003.02619.x.
6. **Cenier T, David F, Litaudon P, Garcia S, Amat C, Buonviso N.** 2009. Respiration-gated formation of γ and β neural assemblies in the mammalian olfactory bulb. Eur J Neurosci **29:**921–930. https://doi.org/10.1111/j.1460-9568.2009.06651.x.
7. **Chapuis J, Cohen Y, He X, Zhang Z, Jin S, Xu F, Wilson DA.** 2013. Lateral entorhinal modulation of piriform cortical activity and fine odor discrimination. J Neurosci **33:**13449–13459. https://doi.org/10.1523/JNEUROSCI.1387-13.2013.
8. **Chery R, Gurden H, Martin C.** 2014. Anesthetic regimes modulate the temporal dynamics of local field potential in the mouse olfactory bulb. J Neurophysiol **111:**908–917. https://doi.org/10.1152/jn.00261.2013.
9. **David FO, Hugues E, Cenier T, Fourcaud-Trocmé N, Buonviso N.** 2009. Specific entrainment of mitral cells during gamma oscillation in the rat olfactory bulb. PLOS Comput Biol **5:**1–19. https://doi.org/10.1371/journal.pcbi.1000551.
10. **Engel AK, Fries P, Singer W.** 2001. Dynamic predictions: oscillations and synchrony in top–down processing. Nat Rev Neurosci **2:**704–716. https://doi.org/10.1038/35094565.
11. **Fontanini A, Bower JM.** 2005. Variable coupling between olfactory system activity and respiration in ketamine/xylazine anesthetized rats. J Neurophysiol **93:**3573–3581. https://doi.org/10.1152/jn.01320.2004.
12. **Fontanini A, Katz DB.** 2008. Behavioral states, network states, and sensory response variability. J Neurophysiol **100:**1160–1168. https://doi.org/10.1152/jn.90592.2008.
13. **Fu Y, Guo L, Zhang J, Chen Y, Wang X, Zeng T, Ma Y.** 2008. Differential effects of ageing on the EEG during pentobarbital and ketamine anaesthesia. Eur J Anaesthesiol **25:**826–833. https://doi.org/10.1017/S0265021508004687.
14. **Fuentes RA, Aguilar MI, Aylwin ML, Maldonado PE.** 2008. Neuronal activity of mitral-tufted cells in awake rats during passive and active odorant stimulation. J Neurophysiol **100:**422–430. https://doi.org/10.1152/jn.00095.2008.
15. **Fourcaud-Trocmé N, Courtiol E, Buonviso N.** 2014. Two distinct olfactory bulb sublaminar networks involved in gamma and beta oscillation generation: a CSD study in the anesthetized rat. Front Neural Circuits **8:**88–99.
16. **Gervais R, Buonviso N, Martin C, Ravel N.** 2007. What do electrophysiological studies tell us about processing at the olfactory bulb level? J Physiol Paris **101:**40–45. https://doi.org/10.1016/j.jphysparis.2007.10.006.
17. **Gelperin A, Ghatpande A.** 2009. Neural basis of olfactory perception. Ann N Y Acad Sci **1170:**277–285. https://doi.org/10.1111/j.1749-6632.2009.04110.x.
18. **Gómez-Villamandos RJ, Martínez C, Navarrete R, Morgaz J, Domínguez JM, López I, Granados MM.** 2013. Romifidine and low doses of tiletamine-zolazepam in dogs. Vet Anaesth Analg **40:**e40–e47. https://doi.org/10.1111/vaa.12054.
19. **Griffin CE 3rd, Kaye AM, Bueno FR, Kaye AD.** 2013. Benzodiazepine pharmacology and central nervous system–mediated effects. Ochsner J **13:**214–223.
20. **Hampton CE, Riebold TW, LeBlanc NL, Scollan KF, Mandsager RE, Sisson DD.** 2019. Effects of intravenous administration of tiletamine-zolazepam, alfaxalone, ketamine-diazepam, and propofol for induction of anesthesia on cardiorespiratory and metabolic variables in healthy dogs before and during anesthesia maintained with isoflurane. Am J Vet Res **80:**33–44. https://doi.org/10.2460/ajvr.80.1.33.
21. **Hunter JD.** 2007. Matplotlib: A 2D graphics environment. Comput Sci Eng **9:**90–95. https://doi.org/10.1109/MCSE.2007.55.
22. **Jackson J, Goutagny R, Williams S.** 2011. Fast and slow γ rhythms are intrinsically and independently generated in the subiculum. J Neurosci **31:**12104–12117. https://doi.org/10.1523/JNEUROSCI.1370-11.2011.
23. **Jones E, Oliphant T, Peterson P.** 2001. [Internet]. SciPy: Open source scientific tools for Python. [Cited 2 November 2020]. Available at: https://www.scienceopen.com/document?vid=ab12905a-8a5b-43d8-a2bb-defc771410b9
24. **Kapoor V, Provost AC, Agarwal P, Murthy VN.** 2016. Activation of raphe nuclei triggers rapid and distinct effects on parallel olfactory bulb output channels. Nat Neurosci **19:**271–282. https://doi.org/10.1038/nn.4219.
25. **Kay LM.** 2003. Two species of gamma oscillations in the olfactory bulb: dependence on behavioral state and synaptic interactions. J Integr Neurosci **2:**31–44. https://doi.org/10.1142/S0219635203000196.
26. **Kay LM, Beshel J, Brea J, Martin C, Rojas-Líbano D, Kopell N.** 2009. Olfactory oscillations: the what, how and what for. Trends Neurosci **32:**207–214. https://doi.org/10.1016/j.tins.2008.11.008.
27. **Kay LM.** 2014. Circuit oscillations in odor perception and memory. Prog Brain Res **208:**223–251. https://doi.org/10.1016/B978-0-444-63350-7.00009-7.
28. **Kay LM.** 2015. Local field potential in olfaction, p 1527–1533. In: Jaeger D, Jung R. editors. Encyclopedia of Computational Neuroscience. New York (NY): Springer. https://doi.org/10.1007/978-1-4614-6675-8_721
29. **Kim EJ, Kim SY, Lee JH, Kim JM, Kim JS, Byun JI, Koo BN.** 2015. Effect of isoflurane post-treatment on tPA-exaggerated brain injury in a rat ischemic stroke model. Korean J Anesthesiol **68:**281–286. https://doi.org/10.4097/kjae.2015.68.3.281.
30. **Ko JC, Williams BL, Smith VL, McGrath CJ, Jacobson JD.** 1993. Comparison of Telazol, Telazol-ketamine, Telazol-xylazine, and Telazol-ketamine-xylazine as chemical restraint and anesthetic induction combination in swine. Lab Anim Sci **43:**476–480.

31. **Ko JC.** 2013. Anesthesia and pain management in dogs and cats: a color handbook. Hong Kong: Manson Publishing.
32. **Lagier S, Panzanelli P, Russo RE, Nissant A, Bathellier B, Sassoè-Pognetto M, Lledo PM.** 2007. GABAergic inhibition at dendrodendritic synapses tunes γ oscillations in the olfactory bulb. Proc Natl Acad Sci USA **104:**7259–7264. https://doi.org/10.1073/pnas.0701846104.
33. **Lang J, Li A, Luo W, Wu R, Li P, Xu F.** 2013. Odor representation in the olfactory bulb under different brain states revealed by intrinsic optical signals imaging. Neuroscience **243:**54–63. https://doi.org/10.1016/j.neuroscience.2013.03.057.
34. **Li AA, Gong L, Liu Q, Li X, Xu F.** 2010. State-dependent coherences between the olfactory bulbs for delta and theta oscillations. Neurosci Lett **480:**44–48. https://doi.org/10.1016/j.neulet.2010.05.093.
35. **Li A, Gong L, Xu F.** 2011. Brain-state–independent neural representation of peripheral stimulation in rat olfactory bulb. Proc Natl Acad Sci USA **108:**5087–5092. https://doi.org/10.1073/pnas.1013814108.
36. **Li A, Zhang L, Liu M, Gong L, Liu Q, Xu F.** 2012. Effects of different anesthetics on oscillations in the rat olfactory bulb. J Am Assoc Lab Anim Sci **51:**458–463.
37. **Lu DZ, Jiang S, Yu SM, Fan HG.** 2014. A Comparison of anesthetic and cardiorespiratory effects of Tiletamine-Zolazepam/Xylazine and Tiletamine-Zolazepam/Xylazine/Tramadol in Dogs. Pak Vet J **34:**63–67.
38. **Lu DZ, Fan HG, Kun M, Song ZL, Ming YS, Sheng J, Wang HB.** 2011. Antagonistic effect of atipamezole, flumazenil and naloxone following anaesthesia with xylazine, tramadol and tiletamine/zolazepam combinations in pigs. Vet Anaesth Analg **38:**301–309. https://doi.org/10.1111/j.1467-2995.2011.00625.x.
39. **Lu DZ, Feng XJ, Hu K, Jiang S, Li L, Ma XW, Fan HG.** 2018. Inductive effect of Zoletil on cystathionine β-synthase expression in the rat brain. Int J Biol Macromol **117:**1211–1215. https://doi.org/10.1016/j.ijbiomac.2018.06.039.
40. **Manabe H, Kusumoto-Yoshida I, Ota M, Mori K.** 2011. Olfactory cortex generates synchronized top-down inputs to the olfactory bulb during slow-wave sleep. J Neurosci **31:**8123–8133. https://doi.org/10.1523/JNEUROSCI.6578-10.2011.
41. **Mast TG, Griff ER.** 2005. In vivo preparation and identification of mitral cells in the main olfactory bulb of the mouse. Brain Res Brain Res Protoc **15:**105–113. https://doi.org/10.1016/j.brainresprot.2005.05.001
42. **Matsutani S.** 2010. Trajectory and terminal distribution of single centrifugal axons from olfactory cortical areas in the rat olfactory bulb. Neuroscience **169:**436–448. https://doi.org/10.1016/j.neuroscience.2010.05.001.
43. **Murakami M, Kashiwadani H, Kirino Y, Mori K.** 2005. State-dependent sensory gating in olfactory cortex. Neuron **46:**285–296. https://doi.org/10.1016/j.neuron.2005.02.025.
44. **Neville KR, Haberly LB.** 2003. Beta and gamma oscillations in the olfactory system of the urethane-anesthetized rat. J Neurophysiol **90:**3921–3930. https://doi.org/10.1152/jn.00475.2003.
45. **Nusser Z, Kay LM, Laurent G, Homanics GE, Mody I.** 2001. Disruption of GABAA receptors on GABAergic interneurons leads to increased oscillatory power in the olfactory bulb network. J Neurophysiol **86:**2823–2833. https://doi.org/10.1152/jn.2001.86.6.2823.
46. **Pedregosa F, Varoquaux G, Gramfort A, Michel V, Thirion B, Grisel O, Vanderplas J, Passos A, Cournapeau D, Brucher M, Perrot M, Duchesnay E.** 2011. Scikit-learn: machine learning in Python. J Mach Learn Res **12:**2825–2830.
47. **Rojas-Líbano D, Kay LM.** 2008. Olfactory system gamma oscillations: the physiological dissection of a cognitive neural system. Cogn Neurodyn **2:**179–194. https://doi.org/10.1007/s11571-008-9053-1.
48. **Scammell TE, Arrigoni E, Lipton JO.** 2017. Neural circuitry of wakefulness and sleep. Neuron **93:**747–765. https://doi.org/10.1016/j.neuron.2017.01.014.
49. **Schoppa NE.** 2006. Synchronization of olfactory bulb mitral cells by precisely timed inhibitory inputs. Neuron **49:**271–283. https://doi.org/10.1016/j.neuron.2005.11.038.
50. **Tsuno Y, Kashiwadani H, Mori K.** 2008. Behavioral state regulation of dendrodendritic synaptic inhibition in the olfactory bulb. J Neurosci **28:**9227–9238. https://doi.org/10.1523/JNEUROSCI.1576-08.2008.
51. **Tsuno Y, Mori K.** 2009. Behavioral state—Dependent changes in the information processing mode in the olfactory system. Commun Integr Biol **2:**362–364. https://doi.org/10.4161/cib.2.4.8719.
52. **van der Walt S, Colbert SC, Varoquaux G.** 2011. The NumPy array: a structure for efficient numerical computation. Comput Sci Eng **13:**22–30. https://doi.org/10.1109/MCSE.2011.37.
53. **Welch P.** 1967. The use of fast Fourier transform for the estimation of power spectra: a method based on time averaging over short, modified periodograms. IEEE Transactions on Audio and Electroacoustics **15:**70–73. https://doi.org/10.1109/TAU.1967.1161901.
54. **Wheatley KE, Bradshaw CJ, Harcourt RG, Davis LS, Hindell MA.** 2006. Chemical immobilization of adult female Weddell seals with tiletamine and zolazepam: effects of age, condition and stage of lactation. BMC Vet Res **2:**8. https://doi.org/10.1186/1746-6148-2-8.